

Boosted RF-MEMS capacitive shunt switches

X. Rottenberg, H. Jansen[†], B. Nauwelaers*, P. Fiorini, W. De Raedt and H. A. C. Tilmans

IMEC v.z.w., Division MCP, Kapeldreef 75, B3001 Leuven, Belgium
Tel.: +32.16.28.8101, Fax: +32.16.28.1501, E-mail: xavier.rottenberg@imec.be

[†] Twente University, MESA⁺ Research Institute, Electrical Engineering Dpt.,
PO Box 217, 7500 AE Enschede, The Netherlands

* Katholieke Universiteit Leuven, Electrotechniek Dpt., ESAT-TELEMIC
Kasteelpark Arenberg 10, 3001 Leuven, Belgium

Abstract— This paper reports on novel RF-MEMS capacitive switching devices implementing an electrically floating metal layer covering the dielectric to ensure intimate contact with the bridge in the down state. This results in an optimal switch down capacitance and allows optimisation of the down/up capacitance ratio all of which is not possible with conventional capacitive switches. Simulation data and measurement results are presented clearly indicating the boosted performance characteristics compared to conventional RF-MEMS capacitive switches, in the frequency range from 1 to 30 GHz. Down/up capacitance ratios higher than 450 have been measured implying an improvement of a factor 34 over conventional designs with equal size and using the same materials.

Keywords— RF; MEMS; Switches; Variable capacitor

I. INTRODUCTION

RF-MEMS switches offer great potential benefits over GaAs MMICs and PIN diode switches for application in wireless communication systems [1-3]. Prototype RF-MEMS switches display low loss (<0.4 dB), good isolation (>20 dB), extremely low standby power consumption, excellent linearity (IP3>66dBm), compactness and high levels of integration [2-6]. A typical built-up of a RF-MEMS capacitive switch in a shunt configuration implemented on a CPW (CoPlanar Waveguide) line is shown in Figure 1 [4-6]. The switch consists of a suspended movable metal bridge, which is mechanically anchored and electrically connected to the ground of the CPW.

To first order, the switch can be modeled as a capacitor between the metal bridge and the signal line. In the RF-ON state the bridge is up, hence the switch capacitance is small, hardly affecting the impedance of the line. By applying a DC bias (superimposed on the RF signal) the bridge is pulled down onto the dielectric,

the switch capacitance becomes high and the switch is OFF or in the isolation state.

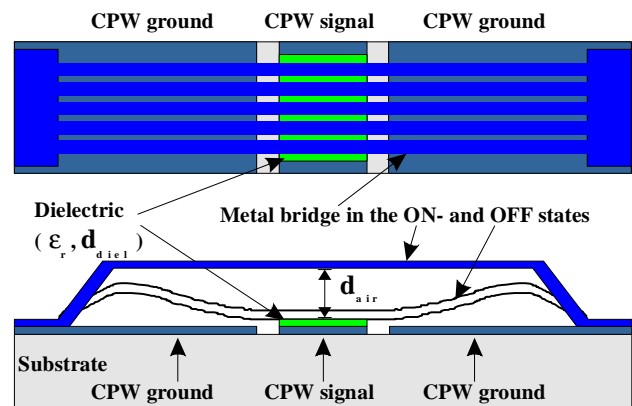


Figure 1: Standard RF-MEMS capacitive shunt switch

An important figure of merit quantifying the RF performance is the down/up capacitance ratio, C_{down}/C_{up} , which must be as high as possible. This ratio can be approximated by the following equation where d_{air} and d_{diel} are the thickness of the air gap and the dielectric, respectively, ϵ_r is the dielectric constant of the dielectric and $A_{overlap}$ is the overlap area of the bridge and the signal line.

$$\frac{C_{down}}{C_{up}} \approx \frac{\epsilon_0 \epsilon_r \frac{A_{overlap}}{d_{diel}}}{\epsilon_0 \frac{A_{overlap}}{d_{air}}} = \epsilon_r \frac{d_{air}}{d_{diel}} \quad (1)$$

For a given technology, as $A_{overlap}$ cancels in (1), the isolation imposes the insertion loss and vice versa. The design freedom is thus heavily constrained.

A second problem encountered in capacitive switches of the type shown in Figure 1 is the degradation of the effective down capacitance as a result of surface roughness preventing intimate contact between beam and dielectric [5]. Figure 2 shows a close-up, not drawn to scale, of the central part of a conventional capacitive

switch illustrating this problem. Preliminary simulations summarized in Figure 3 show that a peak-to-peak roughness distribution uniform between 0 and 20nm on a 250nm thick dielectric with $\epsilon_r = 25$ (Ta_2O_5) already reduces the achieved down-capacitance by a factor 2.

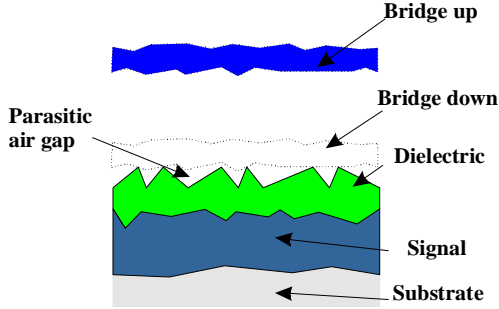


Figure 2: Close-up on the active area of a conventional capacitive shunt switch, clearly showing the parasitic air-gaps as a result of the surface roughness

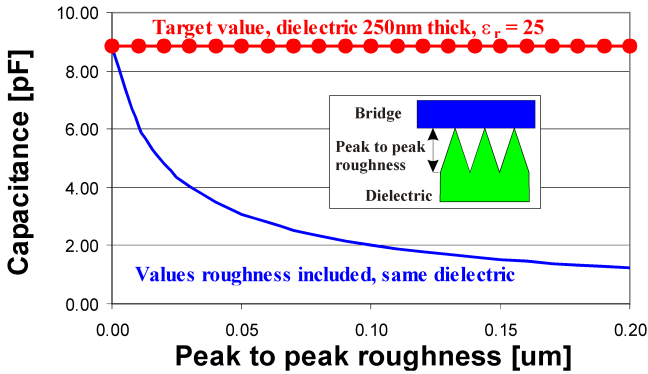


Figure 3: Roughness induced down-capacitance defect.

The commonly pursued solutions to attain a large down capacitance are aimed at keeping the roughness of the bridge and of the dielectric layer very low, e.g., < 5 nm, and to keep the surface free from residues [4-6]. Muldavin *et al.*[5] and Yao *et al.* [6] introduced thin bottom metals in an attempt to reduce the roughness. In particular, in [4], a thin refractory metal layer (e.g., W) was used. All these measures however lead to a high series resistance hence to an increased insertion loss for a shunt switch. Obviously, in a standard design as the one shown in Figure 1, a difficult compromise must be made as methods for improving the isolation directly lead to a deterioration of the insertion loss.

In this paper, a novel RF-MEMS switching structure is introduced in which the isolation is optimised without compromising the insertion loss. In addition a new degree of freedom is introduced to equation (1) that allows us to improve on the standard capacitance ratio by an order of magnitude.

II. SWITCH DESIGN

The basic design is shown in Figure 4. A SEM picture of a fabricated device is shown in Figure 5. Key

in the design is the use of an electrically floating metal layer covering the dielectric.

The concept of using the floating metal is to ensure that an optimal down capacitance can be achieved without having to resort to very smooth surfaces. A few ohmic contact points between the bridge and the floating metal suffice to attain the optimal down-capacitance given by $C_{down} = \epsilon_0 \cdot \epsilon_r \cdot A_{float} / d_{diel}$, where A_{float} is the area of the floating metal. It further allows the use of a thick, e.g., same thickness as usual CPW lines, highly conductive, and thus low-loss bottom metal layer. The only requirement is that the bridge-to-floating metal contact impedance (combination of contact resistance and capacitance due to a native oxide layer) is sufficiently low so as not to limit the best attainable isolation.

As can be seen in Figure 4 and Figure 5, C_{down} is defined by the area of the floating top metal (A_{float}) whereas C_{up} is still determined by the area $A_{overlap}$, the overlap region between the bridge and the signal line, which is independent of A_{float} . This allows further optimising the capacitance ratio. The up-capacitance can be lowered, by choosing a bridge more narrow than the floating top metal, without affecting the down capacitance. We can thus decouple the two switching states and introduce a geometrical factor that “boosts” the capacitance ratio to:

$$\frac{C_{down}}{C_{up}} \approx \frac{\epsilon_0 \epsilon_r \frac{A_{float}}{d_{diel}}}{\epsilon_0 \frac{A_{overlap}}{d_{air}}} = \epsilon_r \frac{d_{air}}{d_{diel}} \frac{A_{float}}{A_{overlap}} \quad (2)$$

The introduction of the floating top metal requires a revision of the actuation scheme of the standard switch of Figure 1. Just covering the dielectric with a floating metal would result in an unstable device. If, in this case, a bias is applied, the bridge pulls in but releases as soon as it touches the floating top metal. Upon contact, the floating top metal and the bridge have the same potential. In other words, the electrostatic attractive force vanishes.

The structure shown in Figure 4 and Figure 5 can be actuated in two ways. One way is via separate actuation electrodes located in area 1 adjacent to the signal line as shown. The other way uses the small areas adjacent to the floating top metal and part of the switch capacitance, indicated as area 2. Using actuation area 1, the capacitive contact can be replaced by an ohmic contact as recently demonstrated by Tan *et al* [7]. In using actuation area 2 a capacitive switch results with the exception that a floating top metal is used. In a final design the actuation area 1 will no longer be used, thus obtaining a very compact capacitive shunt switching device.

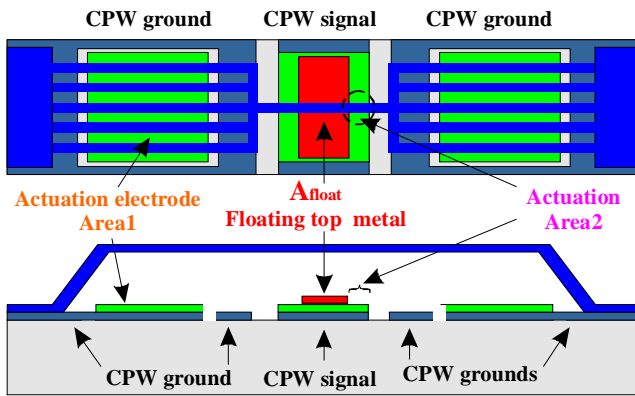


Figure 4: RF MEMS boosted switch.

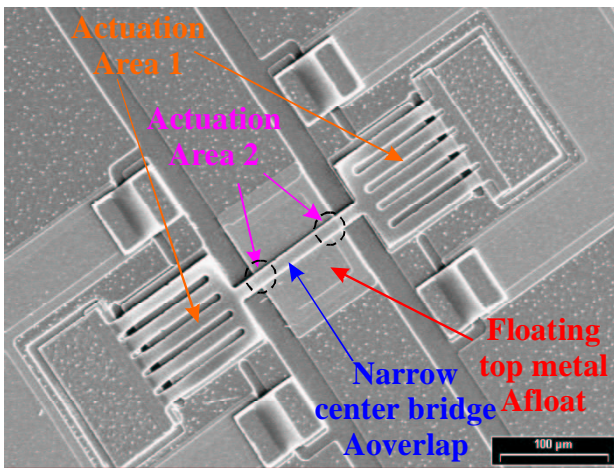


Figure 5: SEM of the boosted RF MEMS switch.

III. PROCESS SEQUENCE

The basic steps of the processing can be described as follows. A stack of $1\mu\text{m}$ Al, 200 nm Ta_2O_5 and 100 nm Al is deposited on a $700\mu\text{m}$ thick AF45 glass substrate. A first mask is used to etch both the top Al and the dielectric to define the area where the bottom Al will be protected. The second mask is used to define the floating top metal plate. The $25/100/25\mu\text{m}$ CPW lines and the top Al for the actuation area 1 are defined with mask #3. Next a $3\mu\text{m}$ thick polymer sacrificial layer is spun and patterned to define the bridge anchors. A $1\mu\text{m}$ Al layer is sputtered and etched defining the bridge. The bridges are released in a final sacrificial layer plasma etch.

IV. SIMULATIONS AND MEASUREMENTS

The $200\mu\text{m}$ long switch areas are fed through $200\mu\text{m}$ long line sections. Figure 6 and Figure 7 show the simulated S-parameters (S_{21}) using HFSS (High Frequency Structure Simulator) for the various switches in the ON-state and the OFF-state, respectively. In Figure 6, a simulation of a $600\mu\text{m}$ CPW line is included for reference purposes.

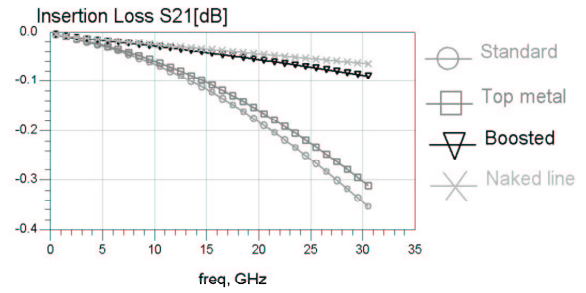


Figure 6: HFSS Insertion Loss simulations of standard switch, switch with floating top metal, boosted switch and naked line

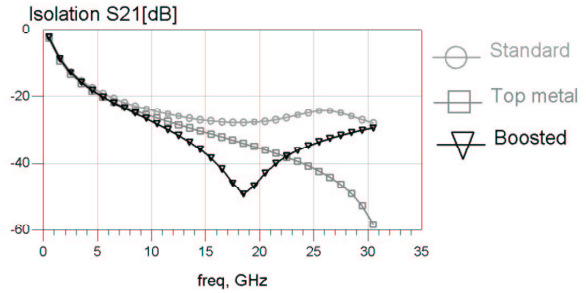


Figure 7: HFSS Isolation simulations of standard switch, switch with floating top metal and boosted switch

The simulations indicate that the same insertion loss is obtained for the standard and the floating top metal devices, but that the boosted switch brings about the expected improvement in the ON-state (bridge in the up-state). The “naked” CPW line is nearly non-sensitive to the presence of a narrow bridge. The loss of the boosted device is only slightly higher than the loss of the naked line (0.09 dB vs. 0.07 dB at 30 GHz for the line).

In the simulations of Figure 7 (switch in down state) a perfect contact between the bridge and the dielectric is assumed. The dip in the curve is well known and is due to the LC resonance [5]. It is found, that the isolation for all structures is the same at low frequencies ($<5\text{ GHz}$). At higher frequencies, the standard switch starts to behave as a number of LC-tanks in parallel, due to the ribbon-like bridge design (see Fig. 1). This broadens the LC resonance dip. The switch with top metal effectively has only a single LC tank giving a single sharp resonance peak. The boosted switch shows similar behaviour but the LC resonance occurs at higher frequency due to the higher inductance of the narrow center bridge. Note that tuning of the LC resonance frequency by shaping the bridge offers the opportunity to greatly improve the isolation in a determined bandwidth. This is of interest for the low frequency application where the shunt switch, by nature, has poor performances.

The insertion loss and the isolation of the various configurations have been measured and are shown in

Figure 8 and Figure 9, respectively. In Figure 9 a fourth curve, labelled as “dummy”, has been added. The dummy represents a bridge permanently fixed during fabrication in the down-state. It is free from any contact problems and represents the optimum bridge shape when pulled down. The dummy is used as the best possible reference to evaluate and compare the actual switches.

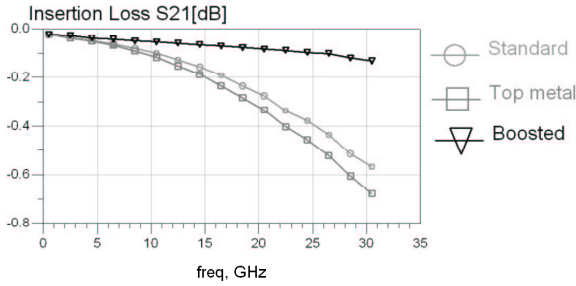


Figure 8: Insertion loss measurements

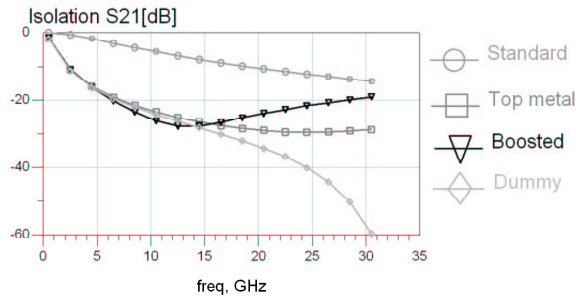


Figure 9: Isolation measurements

The insertion loss measurements show a good agreement with the simulations although different by a factor 2. The source of this discrepancy has not been explained yet. As predicted by the simulations (Figure 6), adding a floating top metal only slightly modifies the behaviour of the switch, increasing the insertion loss with 0.1dB at 30GHz as compared to the standard switch. The boosted switching device shows a much lower loss than the other two device structures. This is explained by the much smaller up-state capacitance of the boosted device. The loss of the boosted switch is now limited by the losses of the 1 μ m thick Al CPW line.

The isolation measurement (Figure 9) on the standard switch shows the typical behaviour of a capacitive switch with poor bridge-dielectric contact. It clearly differs from the simulations. The isolation measurements on the other structures show good agreement with the simulations. They present almost the same low frequency behaviour, the only differences appearing in the LC resonance characteristics. It seems that the dummy structure goes to a sharp LC resonance around 30 GHz, whereas a clear LC resonance is not observed for the other switching devices. The higher series resistance R (see Figure 8) leading to a higher damping and thus a broader dip explains this

observation.

The switches are modelled with the circuit shown in Figure 10. The measurements are fitted on this model using R, L and C as the fitting parameters, with a fixed model for the CPW line sections. The fitting parameters are summarized in Table 1.

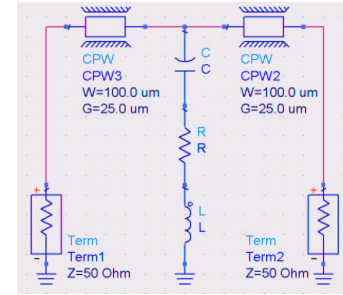


Figure 10: Capacitive shunt switches extraction model

Table 1: Measurement extracted fitting parameters.

	C_{up} [fF]	C_{down} [pF]	L_{down} [pH]	R_{down} [Ω]	$\frac{C_{down}}{C_{up}}$
Standard	68	0.90	(2)	(0.22)	13
Top metal	78	7.98	10	1.12	102
Boosted	18	7.98	18	1.33	459
Dummy	-	9.12	10	0.15	-

The up-capacitance of the standard switch and the switch with top metal do not differ significantly. The boosted switch (with a 5 times narrower center bridge), displays a 4 times smaller up-capacitance. The down capacitance of the top-metallized and boosted switches is the same, and is a factor 9 better than the down-capacitance of the standard switch. The difference between the 7.98 pF measured on the movable structures and the 9.12 pF measured on the dummy structures is due to the difference in contact areas (equal to the “pulling area 2” explained in Figure 4 and Figure 5).

For frequencies (much) smaller than the LC resonance, the capacitance dominates the RLC impedance. The small C_{down} observed for the standard switch shifts the LC resonance to very high frequencies, out of our measurement range. The extracted R_{down} and L_{down} for the standard switch are therefore only poor estimates. For the other configurations, the extracted L- and R-values are more reliable. The inductance for the switch with top metal and the dummy switch is the same, while the boosted switch shows a much higher inductance.

A resistance close to 1 Ω has been extracted for the movable devices using top metal (including the boosted switch), while the dummy shows a much smaller resistance of 0.2 Ω . This can be explained by the thicker top metal of the dummy, which is 1 μ m Al vs. 0.1 μ m thick Al for the other configurations.

Most importantly the calculated capacitance ratio

improves from 13 for the standard switch to above 400 for the boosted device. Truly considered an impressive improvement for the boosted device.

Figure 11 summarizes in a C_{down} vs. C_{up} chart the development of the boosted switch. In this chart, the non-movable dummy switches have been represented as showing a vanishing up-capacitance, thus representing the ideal behaviour sought for a capacitive shunt switch.

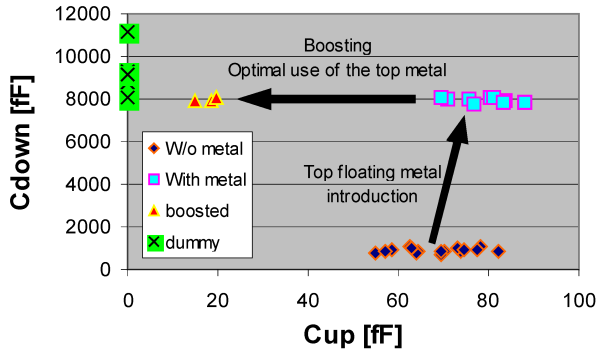


Figure 11: Up- and Down-capacitances improvement

Up- and down-capacitances of the conventional switches differ a lot from their ideal values. With the same dimensions of bridge, the introduction of the top floating metal increases the down-capacitance to its target value, equal to the dummy switch capacitance value. On the chart, the displacement is nearly vertical, as the up-capacitance is almost non-affected. Then, introducing the narrow bridge in the center area shifts the measurements to a region of the chart in a close neighborhood of the dummy switches. The displacement is this time horizontal as only the down-capacitance only is affected.

V. CONCLUSIONS

Novel RF-MEMS capacitive switching devices have been presented. A feature of the devices is that the insertion loss and the isolation can be independently optimised, something which is impossible for a conventional switch designs. Due to this feature, the devices offer a high down-capacitance and a down-to-up capacitance ratio as high as 450, an improvement with a factor 34 over standard designs. The measured insertion loss is below 0.06dB in the range 1-15GHz (and includes the losses of the 600 μ m long lines estimated to be around 0.04dB). Isolation higher than 25dB at 15 GHz has been measured. It is expected that, based on this concept, further improvements are still possible.

VI. ACKNOWLEDGEMENT

This project was supported by ESA-ESTEC under contract 14627/00/NL/KW. The authors in particular would like to thank François Deborgies and Laurent Marchand from ESTEC for the many fruitful discussions. Further acknowledgements go to all the members of the HDIP and MEMS groups of IMEC and especially to Arun Chandrasekhar and Steven Brebels, members of the L.E.T.

VII. REFERENCES

- [1] C. T.-G. Nguyen, L. P. B. Katehi and G. M. Rebeiz, "Micromachined devices for wireless communications", Proc. of the IEEE, vol. 86(8), 1998, pp. 1756-1768.
- [2] J. J. Yao, "RF MEMS from a device perspective", J. Micromech. Microeng., vol.10(4), December 2000, pp. R9-R38.
- [3] G. M. Rebeiz and J. B. Muldavin, "RF MEMS switches and switch circuits", IEEE Microwave magazine, Dec. 2001, pp. 59-71.
- [4] Z. Jamie Yao, S. Chen, S. Eshelman, D. Denniston and C. Goldsmith, "Micromachined low-loss microwave switches", IEEE J. of MEMS, vol. 8(2), 1999, pp. 129-134.
- [5] J. B. Muldavin and G. M. Rebeiz, "High-isolation CPW MEMS shunt switches-Part 1: Modeling", IEEE Trans. Microwave Theory and Techniques, vol. 48(6), 2000, pp. 1045-1052.
- [6] H. A. C. Tilmans, H. Ziad, H. Jansen, O. Di Monaco, A. Jourdain, W. De Raedt, X. Rottenberg, E. De Backer, A. Decaussemaeker and K. Baert, "Wafer-level packaged RF-MEMS switches fabricated in a CMOS fab", proc. IEDM 2001, Washington, DC, December 3-5, 2001, pp. 921-924.
- [7] G.-L. Tan and G. M. Rebeiz, "DC-26 GHz MEMS series-shunt absorptive switches", proc. IEEE MTT-S, Phoenix, AZ, 20-25 May, 2001, pp. 325-328, 2001.